KAUNAS UNIVERSITY OF TECHNOLOGY

FACULTY OF ELECTRICAL AND ELECTRONICS ENGINEERING

DEPARTMENT OF ELECTRONICS ENGINEERING

Variability Investigation of Blood Pressure Estimates Extracted from Photoplethysmogram

Master's Thesis

Biomedical Engineering, 621H16001

Supervisor

(parašas) prof. dr. Vaidotas Marozas

(data)

Reviewer

(parašas) prof. dr. Arūnas Lukoševičius

Author

(parašas) Basant Kumar Bajpai

(data)

KAUNAS, 2015

KAUNAS UNIVERSITY OF TECHNOLOGY

FACULTY OF ELECTRICAL AND ELECTRONICS ENGINEERING

(Fakultetas)

Basant Kumar Bajpai

(Studento vardas, pavardė)

Biomedical Engineering, 621H16001

(Studijų programos pavadinimas, kodas)

Final thesis "Variability investigation of blood pressure estimates extracted from Photoplethysmogram"

ACADEMIC HONESTY DECLARATION

2016 January 10

Kaunas

I **Basant Kumar Bajpai,** confirm that my, final project on "Variability investigation of blood pressure estimates extracted from Photoplethysmogram" is written completely independently and all of the data or results are correct and received honestly. This work does not include of any plaited part from printed or online sources, all other sources of direct and indirect quotes are provided in the list of references. I have not made any illegal payments of money for this work.

I understand if any fact of dishonesty comes to a light, I will be subjected to penalties on the basis of Kaunas University of Technology procedures.

Basant Kumar Bajpai

(First name, Second name) (signature)

Variability investigation of blood pressure estimates extracted from Photoplethysmogram /supervisor prof. Dr. Vaidotas Marozas; Kaunas University of Technology, Faculty of **Electrical and Electronics Engineering**, department of Electronics Engineering

Kaunas, 2015. 45 pages.

SUMMARY

This research is motivated by the demand for unobtrusive methods to monitor blood pressure variability which emerges as a significant biomarker of cardiovascular control mechanisms. It was shown that short-term blood pressure fluctuations might have a prognostic relevance, predicting organ damage and cardiovascular events. There are evidences of positive correlation between increased blood pressure variability, higher average blood pressure level and age. The mentioned factors may accompany a high risk condition such, as diabetes mellitus. However, until now increased blood pressure variability indexes are not utilized in the clinical practice. One of the preventing factors is unavailability of long-term unobtrusive methods for continuous blood pressure registration. Gold-standard 24h blood pressure monitoring with 15 min intervals provides information on blood pressure fluctuations occurring in the "very low" frequency range, whereas the higher-frequency components of blood pressure variability go undetected and can only be assessed with a beat-to-beat measurement technique. The pulse volume waves unobtrusively registered as Photoplethysmogram is an attractive alternative to represent ongoing changes in the body hemodynamics. The primary goal of the performed research was to investigate correlations between the variability of blood pressure parameters and indexes extracted from the model-based analysis of Photoplethysmogram signal. The algorithms for tracking the systolic edge slopes of Photoplethysmogram were investigated primarily. Parametric models (linear and hyperbolic tangent) were fitted continuously over time to detected systolic edges of the hemodynamic pulses. Algorithms for tracking the extracted parameters over time were developed in Matlab software.

The preliminary results of experiments show small association between extracted Photoplethysmogram parameters and blood pressure variation during the tilt table test. The research explains only a part of the proposed parameters for blood pressure variability; reason for the remaining part is unclear, so further study is required.

Fotopletizmogramos analize grįstų kraujo spaudimo įverčių variabilumo tyrimas / vadovas prof. Dr. Vaidotas Marozas; Kauno technologijos universitetas, Elektros ir elektronikos inžinerijos fakultetas, Elektronikos inžinerijos katedra

Kaunas, 2015, 50 puslapių.

SANTRAUKA

Šio tyrimo aktualumą sąlygoja poreikis monitoruoti kraujo spaudimo parametrų variabilumą, kuris tampa reikšmingu širdies ir kraujagyslių valdymo mechanizmų biomarkeriu . Literatūroje yra duomenų, kad trumpalaikes kraujo spaudimo fluktuacijos gali turėti prognostines vertės prognozuojant organų pažaidą ir kardiovaskulinius įvykius. Yra įrodyta, kad egzistuoja ryšys tarp padidėjusio kraujo spaudimo variabilumo, didesnio vidutinio kraujo spaudimo lygio ir amžiaus. Minėti faktoriai gali nulemti padidintos rizikos būsenas, tokias kaip cukrinis diabetas. Tačiau šiuo metu padidėjusio kraujo spaudimo variabilumo indeksai nėra naudojami klinikinėje praktikoje. Vienas iš trukdančiu faktorių yra ilgalaikių ir patogių nuolatinio kraujo spaudimo registravimo priemonių stoka. Aukso standartu laikomas 24 valandų kraujo spaudimo monitoravimas, kurio metu spaudimas registruojamas 15 minučių intervalais. Tačiau šis metodas pateikia informaciją apie kraujo spaudimo fluktuacijas vykstančias palyginti žemų dažnių diapazone. Aukšto dažnio kraujo spaudimo variabilumo komponentės lieka neįvertintos. Aukšto dažnio kraujo spaudimo variabilumo komponentės gali būti įvertintos tik analizuojant kraujo spaudimą kiekvieno širdies dūžio metu. Pacientui patogiai registruojama fotopletizmograma yra patraukli alternatyva hemodinamikos pokyčiams analizuoti. Šio tyrimo tikslas - ištirti ryšius tarp kraujo spaudimo parametrų ir indeksų išskirtų taikant modeliu grįstą fotopletizmografinio signalo analizę. Visų pirma, ištirti algoritmai vertinantys fotopletizmogramos sistolinio fronto nuolydį. Buvo pritaikyti parametriniai modeliai (tiesinis ir hiperbolinio tangento) sistolinių frontų charakterizacijai hemodinamikos impulsuose. MATLAB aplinkoje buvo sukurti algoritmai parametrų nuolatiniam vertinimui atlikti.

Preliminarūs tyrimo rezultatai parodė silpną koreliaciją tarp išskirtų fotopletizmogramos impulsų priekinio fronto parametrų ir kraujo spaudimo parametrų variacijos. Gauti koreliacijos koeficientai neviršija 0,40±0,13. Tačiau tyrimas turi metodologinę vertę – pasiūlyti nauji būdai įvertinti fotopletizmografinių impulsų priekinio fronto statumui. Kraujo spaudimo paaiškina tik tam tikrą dalį pasiūlytų parametrų variabilumo, likusios variabilumo dalies priežastis neaiški. Reikalingi papildomi tyrimai.

Acknowledgement

This master thesis has been carried out at the faculty of electrical and electronics engineering, Kaunas university of technology. A number of people deserve thanks for their support and help. It is therefore my greatest pleasure to express my gratitude to them all in this acknowledgement. First of all, I would like to convey my warmest gratitude to my supervisor Professor Vaidotas Marozas, who gave me the opportunity to conduct my study in his research group and for their guidance, generous contribution of knowledge and experience, valuable comments and encouragement from the start until the end of my study for the language corrections made on my thesis paper. I am thankful to doctoral student Andrius Rapalis for sharing some of his database and I was really privileged to have him for suggestions. I want to thank Andrius Sakalauskas (PhD candidate) for help me in translating my master thesis summery in Lithuanian language, also for enlightening and joyful discussions about social life, science and your invaluable help during the use of Matlab and article sharing. I am also thankful to Ana Rodrigues (Biomedical Maters student) at Department for her help, support use laboratory instruments. I wish to thank my colleagues and friends at the faculty of electrical and electronics engineering for sharing me numerous coffees, lunches, and laugh at all times.

CONTENTS

ABBREVIATIONS AND GLOSSARY

PAP*:* Peripheral arterial pressure

PPG: Photo plethysmography

PDA: pulse decomposition analysis

PAT: Pulse arrival time

BP: Blood pressure

ABPM: ambulatory blood pressure monitoring

BPV: blood pressure variation

PTT: Pulse transit time

INTRODUCTION

When our heart beats and blood pumped into body, blood moves and gives a pressure to the wall of the blood vessels that strength of this pressure is called blood pressure (BP). Ideally a normal blood pressure is 120/80 systolic (highest pressure)-diastolic pressure (lowest pressure), but when these normal pressure varying in ranges of higher and lower numbers such as 140 systolic and 100 diastolic situation called hypertension, similarly less than normal blood pressure causing hypotension see in Figure 1.These pressure fluctuate from normal to high time by time called blood pressure variation. BP variability is also defined as the average variation of BP throughout the day, quantitated as the standard deviation of ambulatory BP. It is increased in hypertensive individuals and increases with aging.

The measurement of BPV is helpful to understand and diagnose the function of the cardiovascular system, various indirect methods of measuring BP such as Riva-Rocca's, oscillometric, ultrasound, and tonometry. Different non-invasive methods utilizing PPG wave analysis devices. Such measurements reveal the systolic pressure in a specific instant of time. These methods do not require inflation and following deflation, which is time consuming and prevents continuous measurement. Moreover, for convenient measurements, the time interval for measurements should be at least 2 minute.

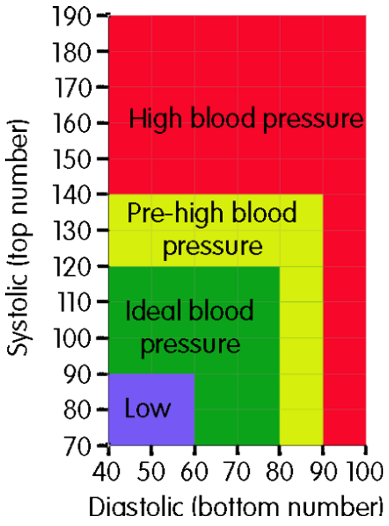

Figure 1 Blood pressure chart[1]

[1] http://www.bloodpressureuk.org

While during some invasive electrophysiology procedures, to continuously monitor arterial blood pressure of an intra-arterial line procedure enhance the risk of complications due to the vascular surgery, an increase of the procedural time, that causes discomfort to the patient. Continuous (beat-to-beat) non-invasive BP measurement is most common in research, anesthesiology, and tilt research labs. The devices use the method to record the arterial waveform indirectly from a finger.

1 LITERATURE ANALYSIS

1.1 Motivation for blood pressure variability analysis

There are strong relations between blood pressure and cardiovascular diseases which represents 50% of the world's cause of death by CV diseases [1].The normal pattern of blood pressure is decrease of around10%−20% during the night, which resemble with hours of sleep, and is referred to as dipping. While a non-dipping pattern is seen in which the normal night sleep fall of pressure is absent. In order to recognize dipping and non-dipping pattern SBP, DBP and mean blood pressure (MBP) taken account that is accurately accessed by 24-hour ambulatory monitor. So, mean arterial pressure (MAP) used as the BP index for confirmation of dipping status [2]. Therefore to recognize dipping and non-dipping pattern of BP, various methods are there we can use diary card entry method. Where we observe the10% cut off fall of sleep time BP for dippers, if it's less than 10% cut off in sleep time BP, person is non-dipper. Studies have showed no dipping pattern is associated with CV diseases, such as left ventricular hypertrophy, increased proteinuria, secondary forms of hypertension, [3].

However, BP is a very unstable parameter and its variability also taken account to be a separate independent risk factor itself [4]. On other hand traditional methods of monitoring BP is limited measurement of systolic and diastolic blood pressure at intervals [5]. So far we have 24-hour ambulatory monitor to get to know about these dipping non dipping pattern and variability. So the development of a 24 hour ambulatory system for continuously monitoring of BP gives deeper insight and proper understanding of the system for blood pressure variability. Moreover, device would help predicting serious cardiovascular events and making anti-hypertensive [5]. While it has certain drawbacks so we need to have unobtrusive method, such as, wearable devices. From a different way, wearable device technology has been advances over the years, especially in recording and processing electrocardiographic (ECG) signals of the acquired ECG data [6]. In Integrating this

system with plethysmography (PPG) signals it could be possible to measure BP indirectly, using the pulse transit time (PTT). Wearable devices a feasible and comfortable way of monitoring patients over long periods of time, provide a significant medium to prevent cardiovascular diseases and improve life expectancy worldwide.

1.2 Existing methods for pressure variability registration

For blood pressure variation monitoring cuff-based 24-hour ambulatory blood pressure monitors Figure 2 is in the trend to use for problems such as dipping and non-dipping, hypertension blood pressure variation.

Figure 2 BP and ECG Holter monitor (a),
24 hour ambulatory blood pressure monitoring [2] (b),

24-hour ABPM is a self-operated device that recorded BP by using the oscillometric method and gives rate of heart variability over 30 minutes for 24 hours. Average BP of sleep BP measured, the time patient came in to bed and till the time patient move of bed and also awaken BP, average BP measurement recorded during day. With this device nocturnal SBP fall calculated with, 100*[1-sleep SBP/day time SBP ratio]. Differentiate the patients with the nocturnal fall, extreme dippers when nocturnal SBP fall is ≥ 20%, dippers when the fall is ≥10%, no dippers when it is ≥ 0% [7].

This device removes biasness and gives information on BP levels and heart rate all the day. The big recordings obtain during the patient's activities provides true BP, also helpful for the diagnosis of hypertension. In addition 24-h ABPM gives outcome on BP variability, circadian changes, and the

[2] http://www.vectordiagnostics.ca/blood-pressure-monitor/

effects of environmental and physical conditions on BP levels. Better accuracy obtains in ABPM with intra-arterial measurements and mercury column sphygmomanometers [8]. 24-h ambulatory monitor giving better correlations with cardiovascular outcome than clinic BP Level.

Commercial availability of Holter type BP devices is presented in Table 1

Table 1 Commercial 24h ambulatory monitors

Product Name	Function type	Product Description	Price Range
Holter with CUFF (CM1203)	ambulatory NIBP data can be recorded once	•Compact and portable, friendly interface, • Patient range: adult, pediatric.	$479.95
CONTEC Abpm50	Ambulatory NIBP data can be recorded once.	• Patient range: adult, pediatric, neonatal	$195.80 ($195)
MD200A	Alarm method: audio, visual (color reverse display).	Manual and auto mode. In auto mode measuring in preset time interval Power: 1.5V Alkali Battery	$399.00
Nibp Monitor	Ambulatory NIBP data recording once.	Compact, portable, friendly and easy to use	$214

1.3 Problems with existing methods for blood pressure variability

The technique of ABPM has many advantages over other available techniques for blood pressure monitoring, but it has its limitations [8]:

- Causing discomfort, particularly at night during sleep because of cuff see in Figure 2
- Need to use reluctantly by some patients, especially for repeat measurements.

- Cost implications see Table 1 Price range.
- Reproducibility is not perfect.
- Possibility of inaccurate measurement readings while activity.
- Inability to detect genuine art factual measurements

1.4 Cuff-less solutions for blood pressure variability estimation

1.4.1 Sphygmograph

This device used for graphically recording of form, strength, and variations of the arterial pulse, introduced in 1854 by Karl von Vierordt. Used as, non-invasive device to record the pressure pulse wave and measure the blood pressure [9]. There are several signals of Sphygmograph that did not explains the strength of the arterial pulse, associated with force over an area of the artery wall that quantify indirectly for the development of the brachial cuff and the auscultator technique to produce the sphygmomanometer [10].

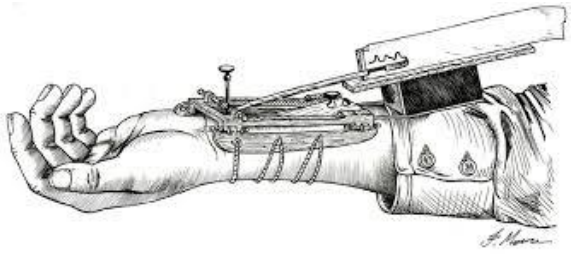

Figure 3 Tridítional E J Marey sphygmograph [10]

The very first recordings of the arterial pulse contour were made in 1863 by E J Marey with Traditional sphygmomanometer Figure 3 was a big wooden device, measure brachial cuff systolic and diastolic pressure used to quantify levels of arterial pressure. To modify the device many scientist explains various method such as from Riva Rocci, palpation method where the brachial cuff is inflated to destroy the peripheral pulse. The cuff slowly deflated till the peripheral pulse is felt at the radial artery. The cuff pressure, where pulse is initially observes as systolic pressure. This method cannot determine diastolic blood pressure. Another Auscultation method described by Korotkoff's observes sounds with the stethoscope placed over the brachial artery change, it shown and disappear as the brachial cuff is slowly deflated. It was useful for systolic blood pressure measurement [10].

Shortcomings of sphygmograph [11]:

- Cuff pressure is dependent on the transduction process, while there fidelity cannot be determined.
- Cuff pressure underestimate true arterial systolic pressure that is independent to device with increased variability at monitoring time.
- Wide variation in pulse pressure observes with scatter in systolic pressure.

1.4.2 Vascular unloading technique – (Penaz Method)

Penaz et al, explained the principle of "unloaded arterial wall", in this method arterial pulsation observed by photo-plethysmography in a finger with a pressure cuff [12]. Instrument based on the volume clamp method of the blood volume under an inflatable finger cuff with an infrared photo plethysmography which is placed inside the cuff, on top of the finger and detector another side that detect and transfer signal to control system that is connected to counter pressure can see in Figure 4.The finger cuff is connected to a small box like device connected to the hand. It has pneumatic valve, a pressure transducer, and electronics for the plethysmography see in Figure 5 a) a traditional TNO Finapres, b) latest Finapres device. The blood volume visualize by the plethysmography is clamped to a set point value by appropriately adjusting cuff pressure in parallel with intra-arterial pressure with an electro pneumatic servo system. This system acquiring the bandwidth of 40 Hz -60 Hz depending on finger cuff size. The volume clamp set point is adjusted to keep the pressure difference across the arterial wall, the pressure [13].

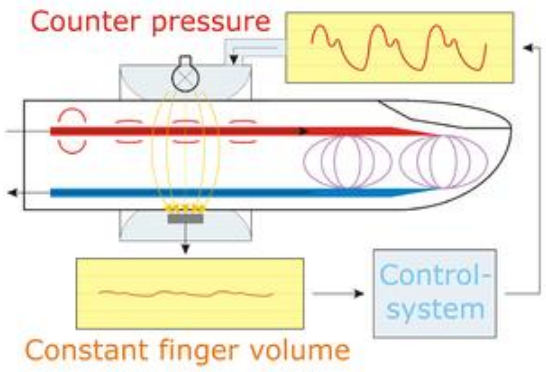

Figure 4 Vascular unloading technique [13]

At zero Tran's mural pressure and cuff pressure same as intra-arterial pressure, indirectly measured by measuring cuff pressure. At this cuff pressure, the veins under the cuff are collapsed. The arteries

under the cuff are not completely closed but open partially to their normal diameter. Thus during systole there is inflow, and during diastole outflow, the fingertip open to the Finapres cuff, for oxygenation in the fingertip [13].

There is a commercial product titled Finapres (Finapres Medical Systems, Hogehilweg 8 NL-1101 CC Amsterdam the Netherlands) using Penaz principle for continuous BP estimation (Figure 5) Finometer PRO has been validated using the Rica-Rocci Korotkoff method because Intra-arterial pressure lower down 5 to 10mmHg in brachial artery if we compare with Riva Rocci, Korotkoff's to Penaz method [14].

a) b)

Figure 5 Traditional TNO Finapres model (a), Finometer PRO current model (b)[3]

1.4.3 Digital CNAP-technology

Continuous non-invasive AP (Arterial pressure) measurements by a new device called CNAP TM (CN Systems Medizintechnik AG, Graz, Austria) commercially available. Figure 6 showing cuff with two arterial site with finger gives oscillometric measurements with detection of fast changes in AP during interventional endoscopy. This device monitors blood pressure also on volume clamp method, in finger. Where blood flow oscillations sensed by the finger cuff to continuous pulse pressure waveforms and beat-to-beat values of AP [14]

[3] http://www.finapres.com/Products/Finometer-PRO

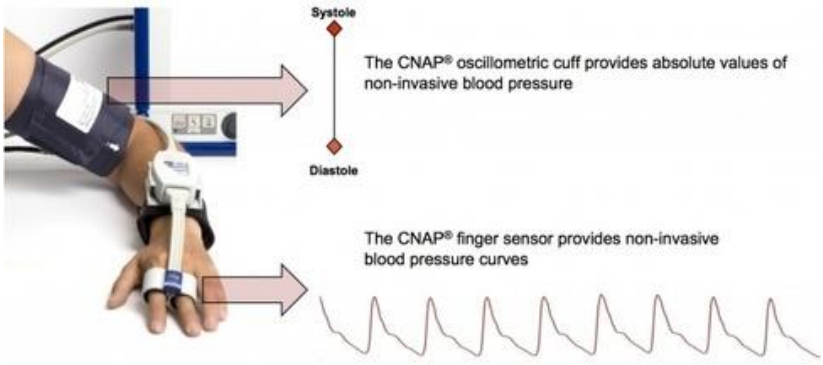

Figure 6 Finger and translates blood flow oscillations in CNAP [14]

Shortcomings of CNAP [15]:

- Since AP changes during the measurement period may increase the size of the measurement error.
- This evaluation protocols may partly not be applicable to continuous non-invasive AP measurements.

1.4.4 Tonometry

Tonometry gives a good, non-invasive assessment of the central pulse pressure waveform. Tonometry means "measuring of pressure," associated aplanation means "flatten." Radial artery is measuring blood pressure by a hand based tonometer that is a strain gauge pressure sensor placing on the radial artery and giving slow pressure to little flatten the artery see in Figure 7 [16]. The radial artery pressure, transmitted from the vessel to the sensor that recorded. A formula using a fast Fourier transformation gives an algorithm that calculates central pressure from a peripheral brachial blood pressure and recording of a PP wave with radial tonometry.

Figure 7 Arterial tonometry [17]

Arterial stiffness measured by tonometry by measuring pulse wave velocity (PWV) and augment index (AIX) by pressure pulse wave analysis (PWA). AT is inexpensive and operator independent alternative [17].

1.4.5 Pulse arrival time (PAT) based blood pressure estimation

Pulse arrival time (PAT) is the time period which is needed for a pulse wave to travel the distance from the heart to any site of the body (e.g. finger, forehead, earlobe, and toe). Measurements of PAT have several applications e.g. estimation of arterial blood pressure, bar reflex sensitivity, cardiac output [18]. Electrocardiogram (ECG) and Photoplethysmogram (PPG) are often used for PAT estimation. There are many definitions of PAT on the basis of the measured time interval (See Figure 8).

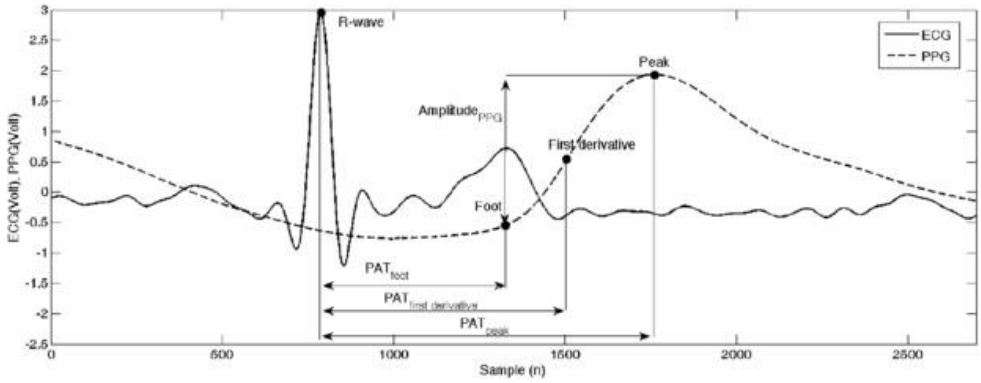

Figure 8 Peak of the ECG R-wave to a fiducially point on the PPG up slope [19]

PAT based on the high quality PPG signal with clearly visible fiducially points on the PPG waveform. However, in case of, orthostatic test subject movement is involved [19]. V. Marozas et al, compare two PAT estimation methods phase shift estimation between fundamental frequency components of ECG and PPG signals concluded new method to estimate PAT during orthostatic test [19].

Photoplethysmogram is ‘plethysmos’ which means increase and ‘graph’ is word for write, and is an instrument used to determine variations in blood volume changes or blood flow with every heartbeat. The PPG signal shows the blood movement in the vessel, which goes from the heart to the fingertips or toes in a wave-like movement, depends on the amount of the backscattering of light shows the variation of the blood volume see in Figure 9 [20].

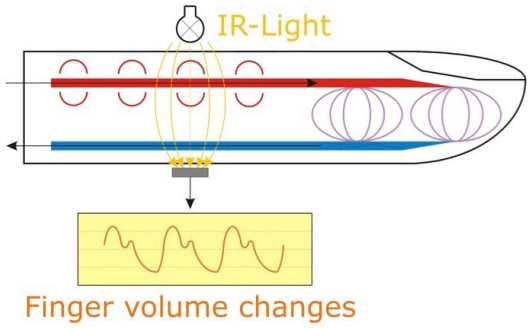

Figure 9 Photoplethysmogram method [20]

It is affected by the heartbeat, the hemodynamics and the physiological condition occurred by the changes of an arteriole properties.

1.4.6 Pulse transit time (PTT) based blood pressure estimation.

Pulse transit time is the time taken by a pulse wave to travel among two arterial sites. Blood pressure directly proportional to the speed of arterial pressure wave travels. A rise in blood pressure causes vascular tone to increase and that makes the arterial wall stiffer causing the PTT shortens [21] an example (See in Figure 10).

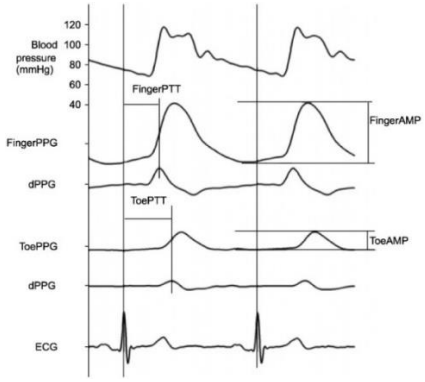

Figure 10 Example of PTT with finger PPG and toe PPG in comparison with ECG [21]

Method from Young explains that PTT decreases as the BP increases. A linear regression equation formed PTT as an input variable establishing the compensation coefficient, after the BP and PTT are measured with inverse relation between the BP and PTT. The systolic and the diastolic BP can be estimated using PTT after the linear regression equation estimating the BP is derived. PTT mostly use data from Photoplethysmogram to Photoplethysmogram.

Similarly Song et al, [22] explain BP measurement with wrist PPG (see in Figure 11) and cuff while the deflation of cuff pressure, the PPG pulse at some point that is similar to Korotkoff sound. When the pulse appeared, the shape of PPG pulses was changed into the certain shape. Thus those points measure the blood pressure.

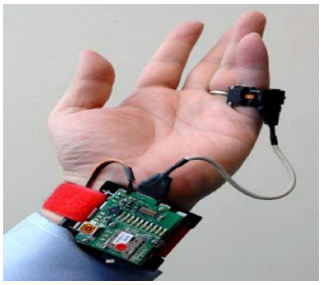

Figure 11 Method of measurement with PTT [22]

Pulse arrival time (PAT),considered as or confuse with PTT but from Zhang G.et al, got that PAT is not an adequate surrogate for PTT in detecting challenging BP changes experiments estimated through the aorta using invasive arterial waveforms [23].

Recently company SOMNOMEDICS introduced commercial device (SOMNO touch NIBP[4]) for BPV monitoring showing the latest ambulatory continuous blood pressure measurement. The blood pressure is measured with the Pulse Transit Time continuously, using an ECG and the SpO2 finger clip additionally to continuous blood pressure, the SOMNO touch NIBP serves as a multi-channel recorder (Figure 12):

Figure 12 Wrist operated SOMNO touch NIBP b) Representation on all body SOMNO touch NIBP[4]

SOMNO touch NIBP gives a continuous blood pressure measurement without inflation of a cuff provides a wide range recording at night sleep time. The continuous recording of the blood pressure shows the minima and maxima, without cuff inflation, disturbs sleep and affects the blood pressure

[4] http://somnomedics.eu/products/new-somnotouch/

advantageous over traditional method. The synchronous recording of movement, sleep and wake measured and blood pressure values can be assigned [24].

1.4.7 PPG pulse analysis techniques

Baruch et al. [25] describes pulse pressure wave analysis called Pulse Decomposition Analysis (PDA). The model explains the peripheral arterial pressure pulse with superposition of five components, the first of which is because to the left ventricular ejection from the heart. Other component are reflections and re-reflections that originate from only two reflection sites within the central arteries T13, the timing delay between the first and third component pulses, correlates correlate with pulse pressure. T13 was monitored with blood pressure, by an automatic cuff and another continuous blood pressure monitor. This model recognizes distinct reflecting arterial tree components to the peripheral pressure pulse envelope [25].

Huotari et al, describe, pulse wave decomposition analysis, with four lognormal wave components. The decomposition occurs after wave computation and fitting compared to the original waves to make sure the best fitting. Comparison and the four lognormal functions used to obtain a residual error curve and their chi-square values describe the goodness of the fit [26].

Elgendi et al, propose algorithm that can detect systolic peaks under challenging conditions accurate systolic-peak detection with heart rate variability (Figure 13). With 40 healthy subjects, gave the best detection accuracy (99.84% sensitivity, 99.89% positive predictivity)[27].

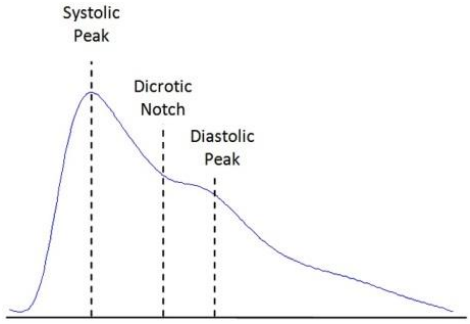

Figure 13 Fingertip photoplethysmogram signal measurement [27]

Augustine et al, explains Pulse height and Pulse width for the Blood Pressure estimation, where systolic amplitude is directly proportional to vascular dispensability with a big range of cardiac output. The systolic amplitude is an indicator of the pulsatile changes in blood volume by arterial

blood flow around the measurement site. It is more suitable measure than pulse arrival time (PAT), systolic amplitude is potentially used for estimating continuous blood pressure [28].

1.5 Aim and Objectives

The literature analysis showed that estimation and monitoring of blood pressure variability is as important as tracking the heart rate variability. Existing methods for blood pressure variability estimation are lacking required time resolution and comfort ability to the patient. Therefore methods for long term unobtrusive monitoring are in crucial demand.

The aim of this work to compare variability of blood pressure parameters (systolic, diastolic, pulse pressure) with their surrogates estimated from photoplethysmogram.

Objectives:

1. To analyze methods for noninvasive estimation of blood pressure parameters;
2. To develop signal processing algorithms for estimation of variability of blood pressure related parameters from photoplethysmogram;
3. To collect data for evaluation of the developed algorithm;
4. To evaluate the performance of implemented algorithm and discuss the results.

2 ANALYSIS OF EFFECTS OF BLOOD PRESSURE ON SYSTOLIC EDGE OF PPG PULSE

2.1 Effect of rising edge in different age of people

Zahedi et al. described a windkessel model to verify the effect of PPG pulse rising edge and peak position. He has chosen 20 to 59 years old subjects, on the basis of PPG amplitude and systolic diastolic pressure, found peripheral pulse shows steep rise and early peak in young subject, on other hand slope becomes blunted in older age people as we can see in Figure 14 [29] it’s slowly becoming blunted in different age people.

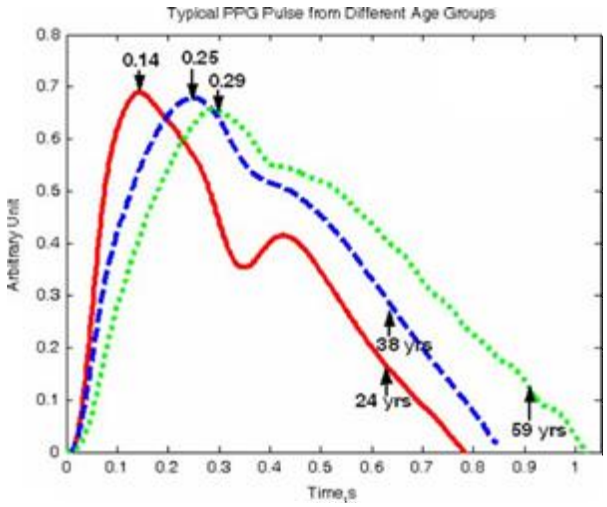

Figure 14 Single PPG pulse, three selected subjects [22]

The Windkessel model (McDonald 1974) is describe hemodynamics relationship between aortic blood flow and pressure in vascular system. Circuit work like a first-order low-pass filters (Figure 15). Such a filter transfer stepwise changes in pressure with some delay, Zahedi et al, [29] chosen the signal for analysis and its recording location.

Various scientists use such circuit for describe the blood flow system through the heart, organs and supplying vessels [6]. In Figure 15 each segment has been calculated based on relating diameter, length and thickness of vessels. Left-ventricular pressure (LVP) is considered as a variable frequency sine wave source; diode as the aortic valve, which shows one directional blood flow. Every section characterized by a proximal resistance (r), an iterance (L) and compliance (C). While Rp represents the peripheral resistance. PSPICE (MicroSim, Corporation) simulate the circuit response to LVP that converts all the biological units into electrical unit [22].

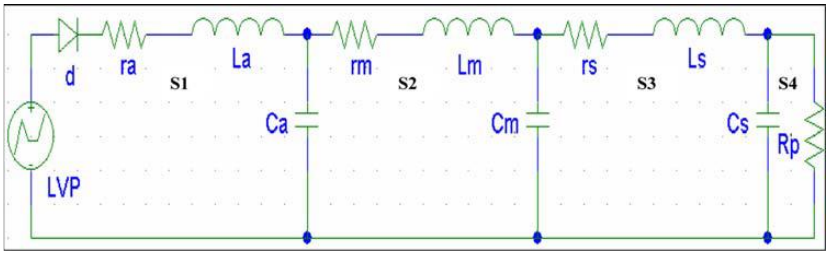

Figure 15 10-Elements Windkessel model [22]

2.2 Effect of vascular changes on the PPG signal at different hand elevations

Hickey et al, explains venous and arterial effects from the photoplethysmographic signal PPG signals from the left index finger. On the hand to 50 cm under heart level, ac and dc both PPG amplitudes from the finger decreased. While, on raising the arm above heart level ac and dc PPG amplitudes increased see in Figure 16 [30].

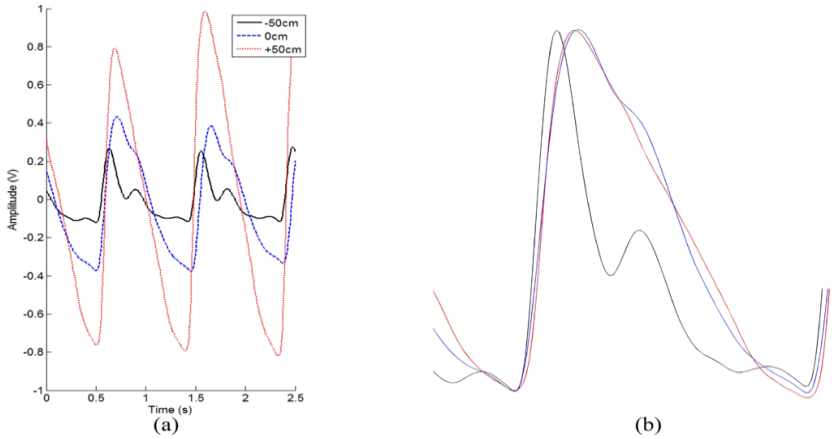

Figure 16 (a) the unaltered PPG signals and (b) PPG signals approximately the same amplitude [30]

In systolic phase Figure 16 we can see that all three waveforms representing sharp systolic peak. However, the time from the foot of the wave to the systolic peak is less when the hand is at −50 cm than at heart level or elevated by 50 cm. [30].

In the diastolic phase there are sharp differences the diastolic slope in the −50 cm PPG signal declines rapidly from the systolic peak from the heart level position dichroitic notch is visible Figure 16 b). At heart level, a fluctuation point, related with the diacritic notch and peak, is visible, while in the elevated position the dichroitic notch is not clearly visible and not differentiable from the systolic peak. At heart level PPG ratio of the diastolic peak to the systolic peak is higher.

2.3 Nonlinear relationship between diameter of the artery and blood pressure

Dhawan et al. [31] explain the diameter of arteries increased with increasing intraluminal pressure. Where, at normal pressures, the ratio of change in diameter: change in pressure was significantly lower in arteries effect in repeatedly breed RB than from age-matched virgins rats Figure 17.

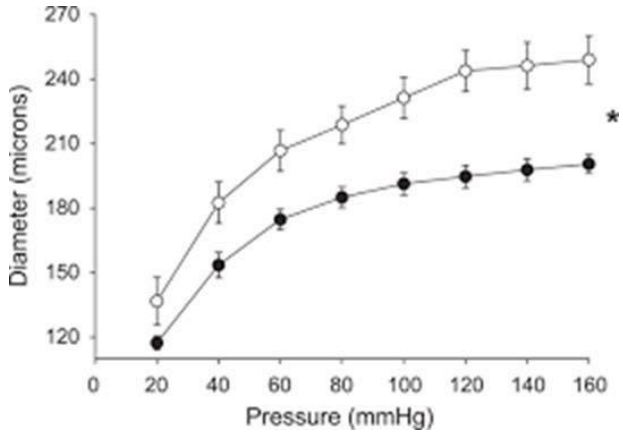

Figure 17 Blood vessel diameter versus blood pressure [20]

Similarly Jessica et al [32], explains in wild type (WT) and mice with one elastin allele younger ones have Vessel inner diameters are similar at physiological blood pressures in comparison of aorta inner diameters of adult WT and Eln mice Figure 18. So increasing arterial inner diameter with an increase in blood pressure is necessary to maintain cardiac output green lines show the diameter of the wild type artery at physiological systolic (S) and diastolic (D) pressures.

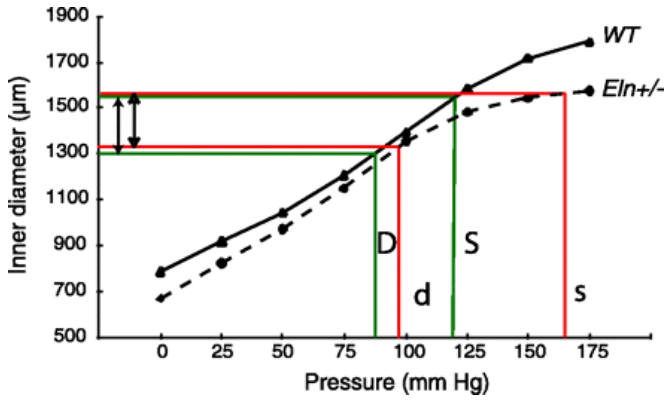

Figure 18 Blood vessel diameter versus blood pressure in younger and older mice [32]

Where from Zahedi et al. described increase in the arterial blood volume dV, is increase the arterial blood pressure (dP). The compliance will decrease with age progression because of changes in the elastin and collagen content of the arterial wall [29].

So similarly we assume as pressure increases diameter increases but until saturation where diameter stops increasing. The parameter values for every section have calculated based on equations of diameter, length and thickness of blood vessels [29].Arterial rigidity can be characterized by the arterial compliance C, defined by (1)

$$c = \frac{dV}{\Delta P} \tag{1}$$

Suppose we have compliance C1 (2) and C2 (3)

$$C1 = \frac{\Delta d1}{\Delta p} \tag{2}$$

$$C2 = \frac{\Delta d2}{\Delta p} \tag{3}$$

$$\Delta V1 = \Delta d1.L > \Delta d2. = \Delta V2 \tag{4}$$

$$c1 = \frac{\Delta v1}{\Delta P} > C2 = \frac{\Delta v2}{\Delta P} \tag{5}$$

From (5) and Figure 17 we can see compliance c1 higher at lower pressure and c2 lower at higher pressure. So we could conclude for different age people, in different age group compliance will be different Such as in older people due to rigidity in their wall compliance will be higher while in middle age people its moderate and in young people less so diameter will be big gives rise sharp peak in pulse peak [29]. Here arbiter unit showing volume as we also mention older people having less or smaller peak can see in Figure 14 because of rigidity in arterial wall. Similarly young people have high volume because of less rigid wall.

3 SYSTOLIC EDGE SLOPE ESTIMATION ALGORITHMS

3.1 Preprocessing

ECG and PPG signals were band pass filtered with 12-30 Hz and 0.15-20 Hz filters, respectively. We used Pan-Tomkins algorithm for RR intervals detection. These intervals were used for PPG signal segmentation into pulses for subsequent estimation of raising front slopes of PPG pulses.

3.2 Estimates of raising front slope of PPG pulses

3.2.1 Peak position

The first slope estimate was proposed by Zahedi [29] peak position method, peripheral pulse shows a rise in younger subjects. With age, the slope becomes blunted in older people, the rise is slow and the pulse peak appears later (Figure 19). Results were verified by a 10-element Windkessel model.

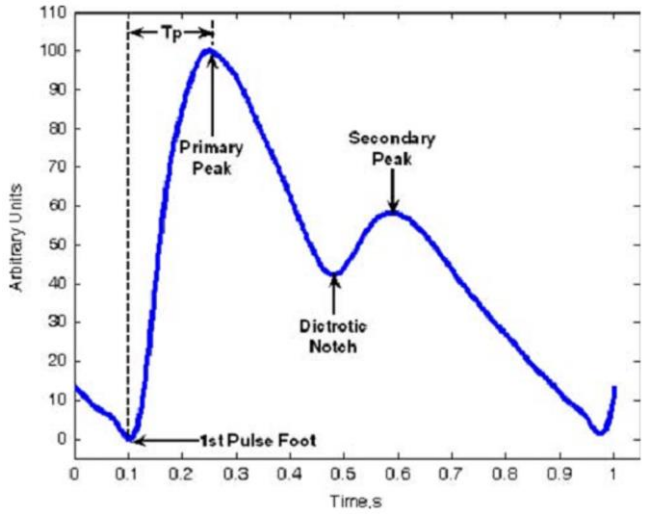

Figure 19 PPG signal pulses definition [22]

3.2.2 PPG derivative-based

The second slope estimate was proposed by Pilt [33], the slope of the PPG signal rising front calculation in Pilt estimation was derived from already existing study by Zahedi et al [29] The first derivative signal *x[m]* (m sample number) it was calculated from the PPG signal *x[m]*. For each return, point m was obtained from the first derivative signal of PPG. Moreover, the amplitude of the PPG signal PPG amplitude was calculated for every recurrence (Figure 20). The slope of the raising front of the PPG signal *Sr* was calculated for each recurrence as:

$$Sr = \frac{x'[m]}{f_d} . \frac{1}{A_{PPG}} \quad (6)$$

Where: $x'[m]$ – the first PPG derivative, A_{PPG} – amplitude of PPG signal pulse, f_d – sampling frequency.

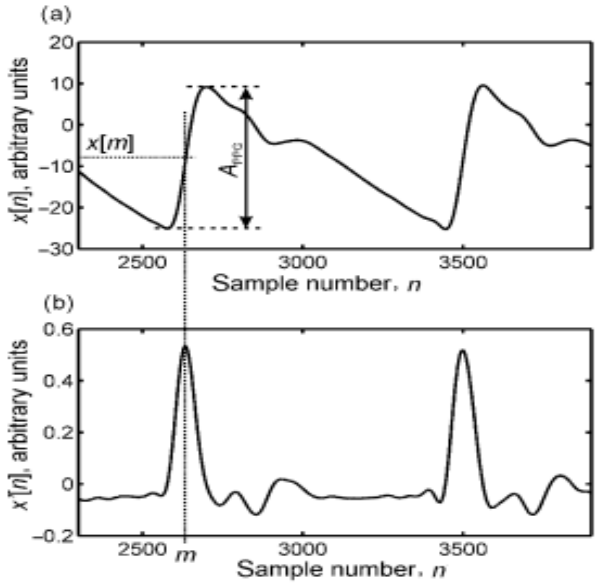

Figure 20 PPG signal x[n] (a) and first derivative of the PPG signal x′ [m] (b) with detected sample number [33]

Raising front of the PPG signal based on the heart rate. With higher heart rate the waveform front tends to increase [29].

3.2.3 Model based estimates

As the third and fourth slope estimates, we propose to parameterize systolic edge with line and hyperbolic tangent functions and to use parameters a and σ as slope parameters:

$$y(n) = \mathrm{a} \cdot \mathrm{n} + b \tag{7}$$

$$y(n) = \mathrm{A} \cdot \tanh\left(\frac{x-\mu}{\sigma}\right) + C \tag{8}$$

Linear parameterization of systolic edges of PPG pulses is exemplified in Figure 21:

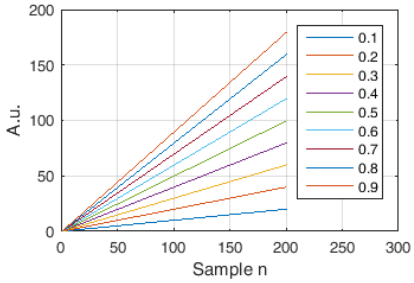

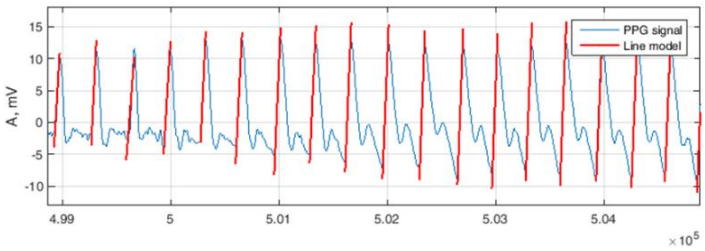

a) b)

Figure 21 Examples: line slope as the function of parameter *a* (a), fitting of the lines to systolic edges of PPG pulses (b)

Hyperbolic tangent parameterization of systolic edges of PPG pulses is exemplified in Figure 21:

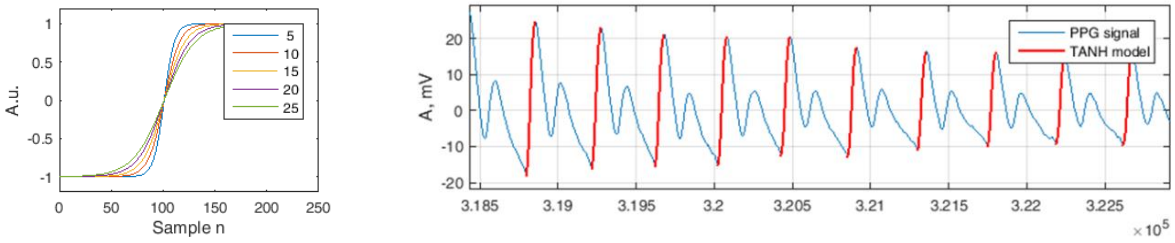

a) b)

Figure 22 Examples: *tanh* functions with changing parameter *σ* (a), fitting of the lines to systolic edges of PPG pulses (b)

In Figure 22 we can see modelling example of systolic edges of PPG pulses with hyperbolic tangent function. Where only the middle part of *tanh* function is used for fitting. The *tanh* function parameters (A, μ, σ and C) are estimated by optimization technique (least squares algorithm). The parameter σ is associated with the slope of systolic edge of PPG pulses and will be used as the surrogate parameter for blood pressure.

4 EQUIPMENT, DATA AND AGREEMENT EVALUATION

4.1 Equipment

Data was acquired by using two synchronized physiological signals recording systems. ECG, PPG and ACC signals were acquired by using Cardioholter6.2-8E78 (BMII, Lithuania) Figure 23 (b). Continuous blood pressures were acquired by a non-invasive continuous finger blood pressure measurement and recording system Portapres Model-2 (Finapres Medical Systems B. V., Netherlands) see in Figure 23.(c) BP signal sampling frequency was 100 Hz. Orthostatic test was accomplished by using a tilt table Canaletto Pro (Ferrox S.r.l., Italy) Figure 23 (a).

a) b) c)

Figure 23 Tilt table Canaletto Pro (a), Cardioholter6.2-8E78 (b), and reference equipment Portapres Model-2 (c)

Table 2 Devices used to record PPG ,ECG and ACC signals with site of recording and sampling frequency

Device Type	**Signal Type**	**Sampling Friequency**	**Site**
Cardioholter6.2-8E78(BMII,Lithuania)	ECG, PPG and ACC	ECG-500Hz, PPG - 250 Hz and ACC - 50	Finger
Portapres Model-2	BP signal	100 Hz	Finger

4.2 Data

Tilt table test data was used to evaluate the proposed methodology. We investigated the recordings from 14 volunteers (10 female, 4 male) aged 19 – 30 years (Table 2). The subjects were recommended not to take any substances that influencing cardiovascular system (alcohol, caffeine) and smoking for 6 h before the examination. They were normal, not obese and not taking medication for the duration of the study.

Table 2 Characteristics of the subjects (mean± standard deviation)

	Subjects (n) =14
Age (year)	25.65 ± 2.50
Height (cm)	174.94±9.96
Weight (kg)	67.47 ± 10.67
BMI (body mass index) (kg/m2)	21.98 ± 2.27

Protocol : The database was recorded during orthostatic test, according to the following protocol: 10 min. in stabilization period (resting in a supine position), 10 min. in early supine position, 1 min. in tilting period, 5 min. in standing position, 1 min. in tilting period, 5 min. in later supine position. The table is slowly tilted by 80 degrees. Synchronous ECG, PPG, accelerometer (ACC) and BP signals were recorded in early supine, standing, later supine and tilting positions. Parameter sequences obtained from measured signals were divided into a five parts: I interval (early supine), II interval (tilting positions 1), III interval (standing), IV interval (tilting positions 2) and V interval (late supine) can see inTable 3 .

Table 3 Data recording during orthostatic test (Protocol), position and time duration

Time Duration	**Position of Test (5-Intervals)**
10 Min	Early supine, I interval
1 min	tilting positions, II interval
5 min	Standing, III interval
1 min	tilting positions, IV interval
5 min	late supine, V interval

4.3 Agreement evaluation

The agreement of different methods for blood pressure variability estimation was evaluated by time (correlation function) and frequency (coherence function) domain analysis.

4.3.1 Maxima of cross-correlation function

Cross-correlations function estimating time domain similarity between time series, used in the analysis of multiple time series. Cross-correlation analysis is a generalization of linear correlation analysis. Measure of the strength of the correlation is given by the correlation coefficient,

$$Rxy(L) = Max\left(\begin{cases} \frac{1}{N}\sum_{K=0}^{N-|L|-1}(Xk+|L|-\bar{x})(yk-\bar{y})\ for\ L<0 \\ \frac{1}{N}\sum_{K=0}^{N-L-1}(Xk-\bar{x})(yk+L-\bar{y})\ for\ L\geq 0 \end{cases}\right) \quad (6)$$

Where N pairs of values (x_K,y_K) and their respective means are $\bar{x}$ and $\bar{y}$. And L is delay, When the two variables x and y are perfectly correlated, r= 1. If they are perfectly anti correlated, r= -1. If they are completely uncorrelated= 0.

4.3.2 Magnitude squared coherence

The magnitude squared coherence estimate is a frequency domain measure. Its values can vary between 0 and 1 and indicates how well the process x corresponds to process y at each frequency. The magnitude squared coherence is a function of the power spectral densities. Suppose cross-power Sxy (e^w) can be interpreted like correlation between x(n) and y(n) at a given frequency. The normalized cross power spectrum is defined in (7):

$$\Gamma xy(e^{\omega}) = \frac{Sxy(e^{\omega})}{\sqrt{Sx(e^{\omega})}\quad\sqrt{Sy(e^{\omega})}} \quad (7)$$

This is known as the coherence function. Normalization is done with the square root of the two power spectra. While, the magnitude coherence squared coherence is given in (8):

$$|\Gamma xy(e^{\omega})||^2 = \frac{|Sxy(e^{\omega})|^2}{Sx(e^{\omega})Sy(e^{\omega})} \quad (8)$$

And its range is defined by (9)

$$0 \leq |\Gamma xy(e^{\omega})||^2 \leq 1 \quad (9)$$

5 RESULTS

5.1 Time domain analysis

In Figure 24 below shows examples of registered multimodal signals for all duration of tilt table test a) ECG signal, b) PPG signal and c) BP signal between 600 to 1000 sec subject is in tilt position, where and excerpts of signals showing during supine position Figure 25a) and tilting positions b). It

can be observed that ECG amplitude does not depend on subject position either in tilting and supine position. While PPG amplitude decreases during tilt position and BP amplitude increases during tilt position.

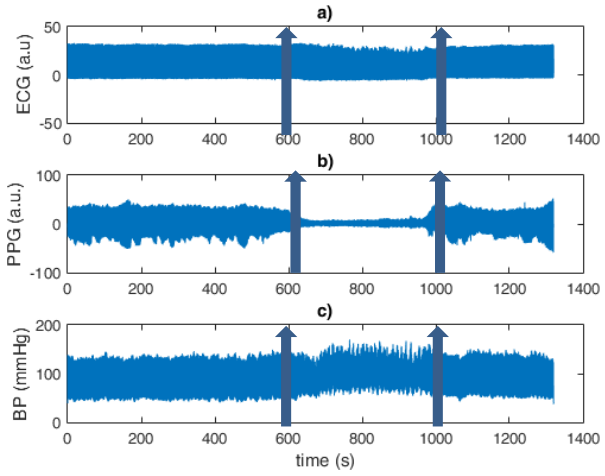

Figure 24 Example of registered multimodal signals for one subject: ECG (a), PPG (b), BP (c)

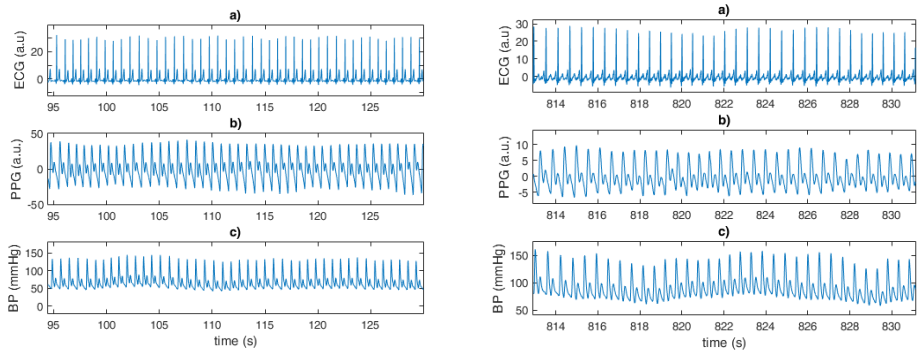

a) b)

Figure 25 Example of registered multimodal signals for one subject: supine position (a) tilt position (b)

Figure 26 shows example of time course of extracted *PPG* and *BP* parameters for one subject where we could observe in a) PAT_{deriv} amplitude decreasing in supine position then increasing in tilt position, in b) PAT_{foot} in tilt position amplitude increasing in tilt position and decreases in supine. In S_{pilt} parameter, amplitude decreases in tilt position. Similarly in parameter S_a, S_σ and *SBP* amplitude increases in tilt position and decreases in supine position while pilt parameter S_{pilt} amplitude is decreasing in tilt position that is not showing ideal calibration.

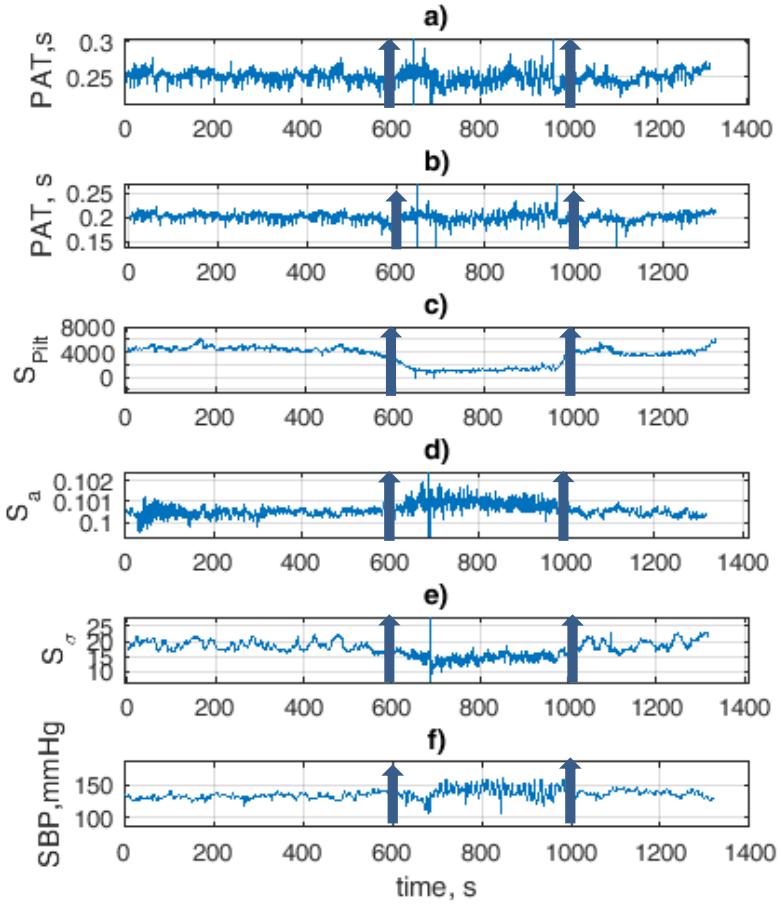

Figure 26 PPG and BP parameters for one subject

Scatter diagram are shown in Figure 27 explaining observed correlation with *SBP*, *DBP* and *BPPP* with all the design parameters and SBP gives quite well correlation prominently with S_{pilt} and *SBP*, while with *DBP* also had good correlation in PAT_{derv} and S_{pilt}. On other hand, *BP PP* was not having very good correlations. So for further estimation of blood pressure scatter diagram showing better correlation of *SBP* with Pilt parameter S_{pilt}, so we could use obtained correlation between *SBP* and S_{pilt} for estimation.

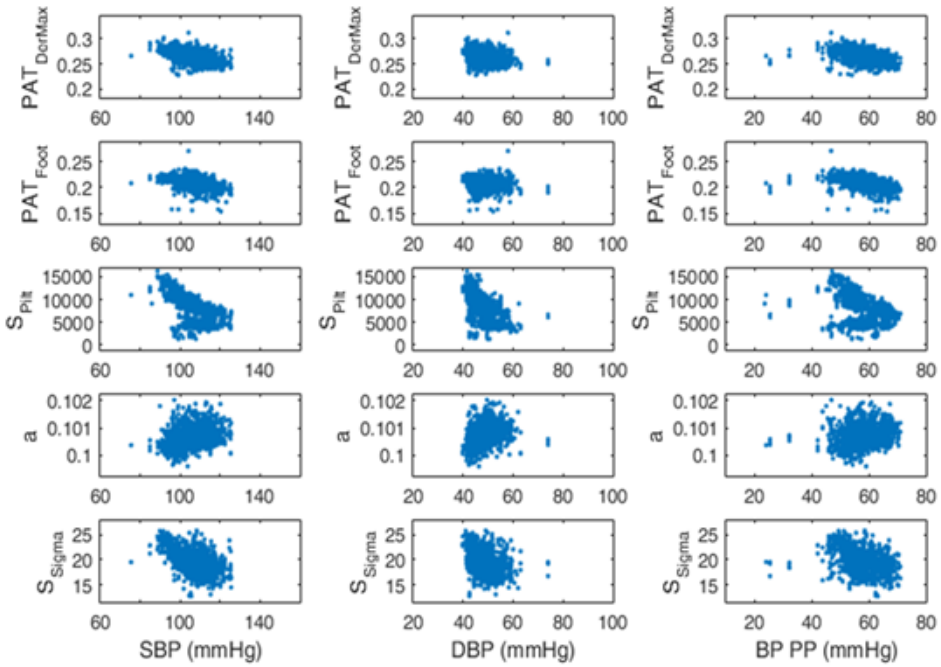

Figure 27 Scatter diagram of SBP, DBP and BP PP with designed parameters

In Correlation matrix shown below in Table 4 between estimates (mean ± std) we have got a strong (positive) linear relationship between PAT_{foot} and PAT_{deriv} with 0.89±0.05 followed by *SBP* and *BP PP* with 0.66±0.18 Similarly a moderate relationship observed in between S_{pilt} and in design parameter S_{σ} with 0.5±0.24.On other hand a correlation found in between *DBP* and *SBP* with 0.59±0.15 and BPPP and S_{Pilt} with 0.40±0.13. Also Pilt parameter and *SBP* with 0.34±0.09, giving a significant correlation result in order to apply for blood pressure monitoring. Remaining our designed parameter with SBP didn't give significant correlation.

Table 4 Correlation matrix (mean ± std)

	PAT_{DerMax}	PAT_{Foot}	S_{Pilt}	S_a	S_σ	SBP	DBP	BP PP
PAT_{DerMax}	1	**0.89±0.05**	0.24±0.12	0.19±0.04	0.11±0.05	0.19±0.08	0.20±0.10	0.19±0.09
PAT_{Foot}	-	1	0.21±0.10	0.01±0.03	0.21±0.06	0.16±0.07	.18±0.09	0.18±0.08
S_{Pilt}	-	-	1	0.31±0.14	**0.54±0.19**	**0.34±0.09**	0.39±0.12	**0.40±0.13**
Sa	-	-	-	1	0.24±0.10	0.26±0.11	0.32±0.17	0.24±0.10
S_σ	-	-	-	-	1	0.26±0.06	0.33±0.15	0.19±0.06
SBP	-	-	-	-	-	1	**0.59±0.15**	0.66±0.18

DBP	-	-	-	-	-	-	1	0.32±0.11
BP PP	-	-	-	-	-	-	-	1

5.2 Frequency domain analysis

Magnitude square can be considered as frequency domain counterpart of cross-correlation coefficient. The magnitude squared coherence for two signals describing heart rate and systolic arterial pressure. From experiment and their result shown in that the two parameters are strongly correlated around 0.1 Hz since the magnitude square coherence is around 0.8, with *SBP* PAT_{Foot} and *SBP* PAT_{derv} had the same coherence. PAT_{Foot} and PAT_{derv} gives good correlation with all the parameters Similarly our designed parameters with *SBP* S_{σ} gives moderate correlated around 0.1 Hz since the magnitude square coherence 0.6 and *SBP* S_a around 0.1Hz since the magnitude square coherence is obtain around 0.5. These results show that our method poorly agrees with the reference method.

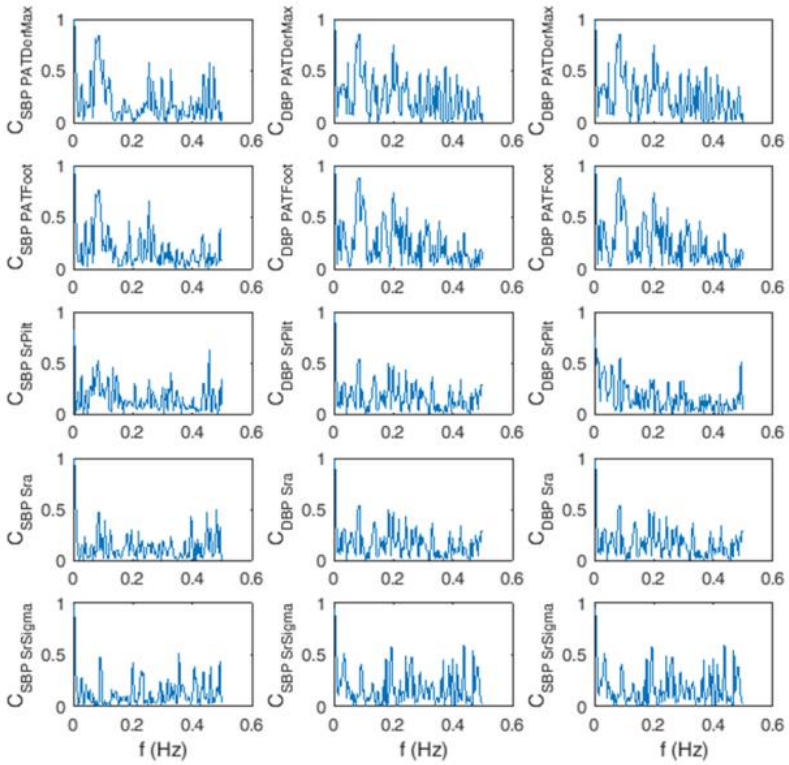

Figure 28 Magnitude squared coherence of designed parameters for one subject

6 DISCUSSION, CONCLUSIONS AND FUTURE DIRECTIONS

Blood pressure variability emerges as a significant biomarker of cardiovascular control mechanisms. Short-term blood pressure fluctuations might have a prognostic relevance, predicting organ damage and cardiovascular events. Until now increased blood pressure variability indexes are not utilized in the clinical practice. The preventing factor is unavailability of long-term unobtrusive methods for continuous blood pressure registration. Gold-standard 24h blood pressure monitoring with 15 min intervals provides information on blood pressure fluctuations but they were unable to detect higher frequencies. Also 24-h ambulatory monitor is not comfortable for sleep.

Photoplethysmogram is an attractive alternative to represent ongoing changes in the body hemodynamics and can be implementable in a wearable device. Different methods were proposed to extract slope-related PPG parameters.

Results show that correlations between the variability of blood pressure parameters and indexes extracted from the model-based analysis of Photoplethysmogram signal, Pilt and Zahedi's estimates are evidences of positive correlation between increased blood pressure variability, higher average blood pressure level and age. Taking in account these two Pilt's and Zahedis rising edge estimation, our parametric models (linear and hyperbolic tangent) are fitted continuously over time to detected systolic edges of the hemodynamic pulses in time domain analysis. Correlation matrix between estimates (mean ± std) show a strong relationship between already known parameters PAT_{foot} and PAT_{deriv} with 0.89±0.05 followed by S_{Pilt} (Pilt parameter) and S_{σ} (0.54±0.19.While in our designed parameter $S\sigma$ and S_a we have got poor correlation with systolic blood pressure was 0.26±0.11and 0.26±0.06 respectively.

In frequency domain analysis, magnitude square coherence signals are strongly correlated around 0.1Hz since the magnitude square coherence is around 0.8, in between *SBP* and PAT_{derv}. Similarly, *SBP* PAT_{foot} correlated around 0.1 Hz since the magnitude square coherence is around 0.8, moreover, our designed parameter S_{σ} with *SBP* showing moderate coherence relation around 0.2 Hz with the magnitude square coherence 0.6. Another side between *SBP* and *Sa* at 0.1Hz, magnitude squared coherence is obtained around 0.5.

From above results, our hypothesis parametric models (linear and hyperbolic tangent) not fit for SBP measurement from correlation matrix results, while there could be some possibility if we look

into magnitude square coherence, that reflect moderate correlation with our designed parameters, showing the small possibilities to use the slope of the PPG signal waveform for parameterize systolic edge with line and hyperbolic tangent functions. On contrary, there could some possibility behind not to obtained better correlations, possibly all the information for correlation could be hidden in frequencies. Also one study for Portapres validation [34] explains that it provides lower correlation in systolic blood pressure than diastolic blood pressure standardizes by British Hypertension Society (BHS, grading A to D), gave B-grade in diastolic BP and C-grade in systolic BP, could also be a reason to obtain lower correlation with SBP from Portapres device.

As a future direction in this research, investigation of different body places for PPG registration (like chest, wrist, ear or forehead) could be proposed.. The correlation of extracted parameters with invasive BP measurements would give definite answer to our hypothesis.

7 BIBLIOGRAPHY

[1] World Health Organization. World health statistics 2012, 2012. URL: http://www.who.int/gho/publications/world_health_statistics/EN_WHS2012_Full.pdf

[2] Birkenhager, A. M., & van den Meiracker, A. H. (2007). Causes and consequences of a non-dipping blood pressure profile. *Neth J Med*, *65*(4), 127–131.

[3] Mahabala, C., Kamath, P., Bhaskaran, U., Pai, N. D., & Pai, A. U. (2013). Antihypertensive therapy: nocturnal dippers and no dippers. Do we treat them differently? *Vascular Health and Risk Management*, *9*, 125–33. http://doi.org/10.2147/VHRM.S33515

[4] Pickering, T. G. (n.d.). Editorial Comment the Clinical Significance of Diurnal Blood Pressure Variations Dippers and Non dippers.

[5] Correia, T. (2012). Integrated Master in Biomedical Engineering Prediction of Critical Blood Pressure Changes Based on Surrogate Measures.

[6] Ferrari, a Physical Mod 2000 IJAO (2). (n.d.).

[7] Elgendi, M. (2012). On the Analysis of Fingertip Photoplethysmogram Signals. *Current Cardiology Reviews*, *8*, 14–25.

[8] Parati, G., Ochoa, J. E., Lombardi, C., Bilo, G., Parati, G., Ochoa, J. E., Bilo, G. (2013). Assessment and management of blood-pressure variability. *Nature Reviews Cardiology*, *10*(10), 143–155. http://doi.org/10.1038/nrcardio.2013.1

[9] Grossman, E. (n.d.). Ambulatory Blood Pressure Monitoring in the Diagnosis and Management of Hypertension. http://doi.org/10.2337/dcS13-2039

[10] P. Avolio, M. Butlin, and A. Walsh, "Arterial blood pressure measurement and pulse wave analysis--their role in enhancing cardiovascular assessment" *Physiol. Meas.*, vol. 31, no. 1, pp. R1–47, Jan. 2010.

[11] Wang, L., Xu, L., Feng, S., Q-H Meng, M., & Wang, K. (2013). Multi-Gaussian fitting for pulse waveform using Weighted Least Squares and multi-criteria decision making method. *Computers in Biology and Medicine*, *43*, 1661–1672. http://doi.org/10.1016/j.compbiomed.2013.08.004

[12] Ogedegbe, G., & Pickering, T. (n.d.). Principles and techniques of blood pressure measurement. http://doi.org/10.1016/j.ccl.2010.07.006

[13] M Imholz, B. P., Van Montfrans, G. A., Settels, J. J., A Van Der Hoeven, G. M., Karemaker, J. M., & Wieling, W. (1988). Continuous non-invasive blood pressure monitoring: reliability of Finapres device during the Va1salva maneuver. *Cardiovascular Research*, *22*, 390–397

[14] G.J M-997-Finapres_rather_than_intra-arterial_or_intermittent_techniques. (n.d.).

[15] Jeleazcov, C., Krajinovic, L., Münster, T., Birkholz, T., Fried, R., Schüttler, J., & Fechner, J. (2010). Precision and accuracy of a new device (CNAP^{TM}) for continuous non-invasive arterial pressure monitoring: Assessment during general anesthesia. *British Journal of Anesthesia*, *105*(3), 264–272. http://doi.org/10.1093/bja/aeq143

[16] C. Liu, D. Zheng, and A. Murray, "Arteries Stiffen With Age, but Can Retain an Ability to Become More Elastic With Applied External Cuff Pressure," Medicine (Baltimore)., vol. 94, no. 41, p. e1831, 2015.

[17] Yong-2010-Estimatiuon of Systolic and Diastolic Pressure using the Pulse Transit Time.

[18] Allen, J., & Murray, A. (2002). Age - related changes in peripheral pulse timing characteristics at the ears, fingers and toes. *Journal of Human Hypertension*, *16*, 711–717. doi:10.1038/sj.jhh.100147.

[19] Rapalis, A., Janušauskas, A., & Marozas, V. (n.d.). Pulse arrival time estimation based on fundamental frequency component extraction.

[20] Dhawan, V., Brookes, Z. L. S., & Kaufman, S. (2004). Long-term effects of repeated pregnancies (multiparty) on blood pressure regulation. *Cardiovascular Research*, *64*(1), 179–86. http://doi.org/10.1016/j.cardiores.2004.06.018

[21] Smith, R. P., Argod, J., Pépin, J. L., & Lévy, P. a. (1999). Pulse transit time: an appraisal of potential clinical applications. *Thorax*, *54*(5), 452–457. http://doi.org/10.1136/thx.54.5.452

[22] Song, S., Cho, J., Oh, H., Lee, J., & Kim, I. (n.d.). Estimation of Blood Pressure Using Photoplethysmography on the Wrist.

[23] Zhang, G., Gao, M., Xu, D., Olivier, N. B., & Mukkamala, R. (2011). Pulse arrival time is not an adequate surrogate for pulse transit time as a marker of blood pressure. *Journal of Applied Physiology (Bethesda, Md. : 1985)*, *111*(6), 1681–6. http://doi.org/10.1152/japplphysiol.00980.2011

[24] Birkenhager, A. M., & van den Meiracker, A. H. (2007). Causes and consequences of a non-dipping blood pressure profile. *Neth J Med*, *65*(4), 127–131.

[25] M. C. Baruch, D. E. Warburton, S. S. Bredin, A. Cote, D. W. Gerdt, and C. M. Adkins, “Pulse Decomposition Analysis of the digital arterial pulse during haemorrhage simulation,” Nonlinear Biomed. Phys., vol. 5, no. 1, p. 1, 2011.

[26] Huotari, M., Maatta, K., & Kostamovaara, J. (n.d.). Radial artery pulse wave measurement by photoplethysmograpy and compound pulse wave decomposition.

[27] Elgendi, M., Norton, I., Brearley, M., Abbott, D., Schuurmans, D., & Bondarenko, V. E. (2013). Systolic Peak Detection in Acceleration Photoplethysmogram Measured from Emergency Responders in Tropical Conditions. *PLoS ONE*, *8*(10). http://doi.org/10.1371/journal.pone.0076585

[28] Augustine, S. (2013). Non Invasive Estimation of blood pressure using a linear regression model from the photoplethysmogram (PPG) Signal. *International Academic and Industrial Research Solutions (IAIRS)*.

[29] E. Zahedi, K. Chellappan, M. Ali, and H. Singh, "Analysis of the Effect of Ageing on Rising Edge Characteristics of the Photoplethysmogram using a Modified Windkessel Model," Cardiovasc. Eng., vol. 7, no. 4, pp. 172–181, 2007.

[30] M. Hickey, J. P. Phillips, and P. A. Kyriacou, "The effect of vascular changes on the photoplethysmographic signal at different hand elevations." *Physiol. Meas.*, vol. 36, no. 3, pp. 425–40, Mar. 2015.

[31] Dhawan, V., Brookes, Z. L. S., & Kaufman, S. (2004). Long-term effects of repeated pregnancies (multiparty) on blood pressure regulation. *Cardiovascular Research*, *64*(1), 179–86. http://doi.org/10.1016/j.cardiores.2004.06.018

[32] Wagenseil, J. E., & Mecham, R. P. (2009). Vascular extracellular matrix and arterial mechanics. *Physiological Reviews*, *89*(3), 957–989. http://doi.org/10.1152/physrev.00041.2008

[33] Pilt, K., Meigas, K., Kööts, K., & Viigimaa, M. (2014). Photoplethysmographic signal rising front analysis for the discrimination of subjects with increased arterial ageing. *Proceedings of the Estonian Academy of Sciences*, *63*(3), 309–314. http://doi.org/10.3176/proc.2014.3.03

[34] Hehenkamp WJ, Comparison of Portapres with standard sphygmomanometry in pregnancy. http://www.ncbi.nlm.nih.gov/pubmed/12044344

[35] Pilt, K., Meigas, K., Rosmann, M., Lass, J., & Kaik, J. (2008). An Experimental Study of PPG Probe Efficiency Coefficient Determination on Human Body.

8 APPENDIX. MATLAB SOFTWARE

```
clear all
close all
startpath = '.';
[filenr,nk]=uigetfile('.mat','Choose the file',startpath);
dir_file=[nk,filenr];
load([nk,filenr]);
sig_dur=length(EKG)/500;
%% INTERVAL for visualisation
strt_time=0*60*60; % in s
durat=sig_dur;%;%          % in s
%durat=20;
interval_ECG=strt_time*Fs_ekg+1:(strt_time+durat)*Fs_ekg;
interval_PPG=strt_time*Fs_ppg+1:(strt_time+durat)*Fs_ppg;
interval_BP=strt_time*Fs_porta+1:(strt_time+durat)*Fs_porta-1;

%% ECG PPG conditioning and processing
[ecg,time_ecg]=fnECG_processing(EKG(interval_ECG,:),Fs_ekg,
timekg(1,interval_ECG));
[ppg,ppg_dc,time_ppg]=fnPPG_processing(PPG(interval_PPG,:),Fs_ppg,
timppg(1,interval_PPG));
BP=Porta(:,interval_BP)';
hb_IR=ppg(:,7);% forehead IR
hb_R=ppg(:,9); % forehead R
lf_IR=ppg(:,12);% left finger R
lf_R=ppg(:,14);% left finger IR

%% Visualisation of signals
ppg    =lf_IR;  % finger
%ppg    =hb_R; % forehead
ppg    =[resample(ppg,2,1);0]; %to 500Hz
ecg_PAT=ecg(:,3);
BP = resample(BP,1,2);     %to 500Hz
ax1=subplot(3,1,1);
plot(time_ecg,ecg_PAT),title('a)'),ylabel('ECG (a.u)')
ax2=subplot(3,1,2);
plot(time_ecg,ppg),title('b)'),ylabel('PPG (a.u.)')
ax3=subplot(3,1,3);
plot(time_ecg,BP),title('c)'),ylabel('BP (mmHg)')
linkaxes([ax1,ax2,ax3],'x')
xlabel('time (s)')

%% 3 METHODS: PAT estimation methods and parameters
Fs = 500; % standard sampling rate
tic
% LINE parameters
[R_time, RRI, a, b, SBP,DBP,BP_PP]=fnRRI_PAT_LinePrmEst_SBP(ecg_PAT,ppg,BP,Fs);
toc
tic
% TANH parameters
[~, ~, ~, ~, ~, ~, S_r_Sigma, ~, ~, ~, feetTanh, maximaTanh,
ppg_modelTanh,~]=fnRRI_PAT_TanhPrmEst_SBP(ecg_PAT,ppg,BP,Fs);
toc
```

```
tic
% PILT rising front edge
[R_time, RRI, PATDerMax, PATFoot, Rise_time, Pulse_slope,
S_r_Pilt,SBP,DBP,BP_PP,feet,peak]=fnRRI_PAT_Pilt_SBP(ecg_PAT,ppg,BP,Fs);
toc
%% Rezults
n=3;
SBP = medfilt1(SBP,n);
DBP = medfilt1(DBP,n);
BP_PP = medfilt1(BP_PP,n);
figure
set(gcf,'Position',[360 -80 560 698])
% Parameter estimates as the function of time
subplot(3,1,1),plot(R_time,SBP), ylabel('P (mmHg)'),title('SBP'),grid
subplot(3,1,2),plot(R_time,DBP),ylabel('P (mmHg)'),title('DBP'),grid
subplot(3,1,3),plot(R_time,BP_PP),ylabel('P (mmHg)'),title('PP'),grid
xlabel('time, s')
%%
figure
set(gcf,'Position',[360 -80 560 698])
% Parameter estimates as the function of time
subplot(6,1,1),plot(R_time,PATDerMax), ylabel('PAT_{DerMax}
(s)'),title('a)'),grid
subplot(6,1,2),plot(R_time,PATFoot),ylabel('PAT_{foot} (s)'),ylim([0.12
0.35]),title('b)'),grid
subplot(6,1,3),plot(R_time,S_r_Pilt),ylabel('S_{Pilt}'),title('c)'),grid
subplot(6,1,4),plot(R_time,a),ylabel('S_a'),title('d)'),grid
subplot(6,1,5),plot(R_time,S_r_Sigma),ylabel('S_{\sigma}'),ylim([min(S_r_Sigma)
max(S_r_Sigma)]),title('e)'),grid
subplot(6,1,6),plot(R_time,SBP), ylabel('SBP,mmHg'),ylim([50
150]),title('f)'),grid
xlabel('time, s')

%% Correlations
R1 = max(xcorr(PATDerMax-mean(PATDerMax),PATFoot-mean(PATFoot), 'coeff'))
R2 = max(xcorr(PATDerMax-mean(PATDerMax),S_r_Pilt-mean(S_r_Pilt), 'coeff'))
R3 = max(xcorr(PATDerMax-mean(PATDerMax),a-mean(a), 'coeff'))
R4 = max(xcorr(PATDerMax-mean(PATDerMax),S_r_Sigma, 'coeff'))
R5 = max(xcorr(PATDerMax-mean(PATDerMax),SBP-mean(SBP), 'coeff'))
R6 = max(xcorr(PATDerMax-mean(PATDerMax),DBP-mean(DBP), 'coeff'))
R7 = max(xcorr(PATDerMax-mean(PATDerMax),BP_PP-mean(BP_PP), 'coeff'))

R8 = max(xcorr(PATFoot-mean(PATFoot),S_r_Pilt-mean(S_r_Pilt), 'coeff'))
R9 = max(xcorr(PATFoot-mean(PATFoot),a-mean(a)))
R10 = max(xcorr(PATFoot-mean(PATFoot),S_r_Sigma-mean(S_r_Sigma), 'coeff'))
R11 = max(xcorr(PATFoot-mean(PATFoot),SBP-mean(SBP), 'coeff'))
R12 = max(xcorr(PATFoot-mean(PATFoot),DBP-mean(DBP), 'coeff'))
R13 = max(xcorr(PATFoot-mean(PATFoot),BP_PP-mean(BP_PP), 'coeff'))

R14 = max(xcorr(S_r_Pilt-mean(S_r_Pilt),a-mean(a), 'coeff'))
R15 = max(xcorr(S_r_Pilt-mean(S_r_Pilt),S_r_Sigma-mean(S_r_Sigma), 'coeff'))
R16 = max(xcorr(S_r_Pilt-mean(S_r_Pilt),SBP-mean(SBP), 'coeff'))
R17 = max(xcorr(S_r_Pilt-mean(S_r_Pilt),DBP-mean(DBP), 'coeff'))
R18 = max(xcorr(S_r_Pilt-mean(S_r_Pilt),BP_PP-mean(BP_PP), 'coeff'))

R19 = max(xcorr(a-mean(a),S_r_Sigma-mean(S_r_Sigma), 'coeff'))
```

```
R20 = max(xcorr(a-mean(a),SBP-mean(SBP), 'coeff'))
R21 = max(xcorr(a-mean(a),DBP-mean(DBP), 'coeff'))
R22 = max(xcorr(a-mean(a),BP_PP-mean(BP_PP), 'coeff'))

R23 = max(xcorr(S_r_Sigma-mean(S_r_Sigma),SBP-mean(SBP), 'coeff'))
R24 = max(xcorr(S_r_Sigma-mean(S_r_Sigma),DBP-mean(DBP), 'coeff'))
R25 = max(xcorr(S_r_Sigma-mean(S_r_Sigma),BP_PP, 'coeff'))

R26 = max(xcorr(SBP-mean(SBP),DBP-mean(DBP), 'coeff'))
R27 = max(xcorr(SBP-mean(SBP),BP_PP-mean(BP_PP), 'coeff'))

R28 = max(xcorr(DBP-mean(DBP),BP_PP-mean(BP_PP), 'coeff'))
R = [R1; R2; R3; R4; R5; R6; R7; R8; R9; R10; R11; R12; R13; R14;...
    R15; R16; R17; R18; R19; R20; R21; R22; R23; R24; R25; R26; R27; R28]
%% Scatter diagram
figure
subplot(5,3,1), plot(SBP, PATDerMax, '.'),xlim([60 160]),ylim([mean(PATDerMax)-
3*std(PATDerMax) mean(PATDerMax)+3*std(PATDerMax)]),ylabel('PAT_{DerMax}')
subplot(5,3,4), plot(SBP, PATFoot, '.'),xlim([60 160]),ylim([mean(PATFoot)-
3*std(PATFoot) mean(PATFoot)+3*std(PATFoot)]),ylabel('PAT_{Foot}')
subplot(5,3,7), plot(SBP, S_r_Pilt, '.'),xlim([60 160]),ylim([mean(S_r_Pilt)-
3*std(S_r_Pilt) mean(S_r_Pilt)+3*std(S_r_Pilt)]),ylabel('S_{Pilt}')
subplot(5,3,10), plot(SBP, a, '.'),xlim([60 160]),ylim([mean(a)-3*std(a)
mean(a)+3*std(a)]),ylabel('a')
subplot(5,3,13), plot(SBP, S_r_Sigma, '.'),xlim([60 160]),ylim([mean(S_r_Sigma)-
3*std(S_r_Sigma) mean(S_r_Sigma)+3*std(S_r_Sigma)]),ylabel('S_{Sigma}')
,xlabel('SBP (mmHg)')

subplot(5,3,2), plot(DBP, PATDerMax, '.'),xlim([20 100]),ylim([mean(PATDerMax)-
3*std(PATDerMax) mean(PATDerMax)+3*std(PATDerMax)]),ylabel('PAT_{DerMax}')
subplot(5,3,5), plot(DBP, PATFoot, '.'),xlim([20 100]),ylim([mean(PATFoot)-
3*std(PATFoot) mean(PATFoot)+3*std(PATFoot)]),ylabel('PAT_{Foot}')
subplot(5,3,8), plot(DBP, S_r_Pilt, '.'),xlim([20 100]),ylim([mean(S_r_Pilt)-
3*std(S_r_Pilt) mean(S_r_Pilt)+3*std(S_r_Pilt)]),ylabel('S_{Pilt}')
subplot(5,3,11), plot(DBP, a, '.'),xlim([20 100]),ylim([mean(a)-3*std(a)
mean(a)+3*std(a)]),ylabel('a')
subplot(5,3,14), plot(DBP, S_r_Sigma, '.'),xlim([20 100]),ylim([mean(S_r_Sigma)-
3*std(S_r_Sigma) mean(S_r_Sigma)+3*std(S_r_Sigma)]),ylabel('S_{Sigma}')
,xlabel('DBP (mmHg)')

subplot(5,3,3), plot(BP_PP, PATDerMax, '.'),xlim([10 80]),ylim([mean(PATDerMax)-
3*std(PATDerMax) mean(PATDerMax)+3*std(PATDerMax)]),ylabel('PAT_{DerMax}')
subplot(5,3,6), plot(BP_PP, PATFoot, '.'),xlim([10 80]),ylim([mean(PATFoot)-
3*std(PATFoot) mean(PATFoot)+3*std(PATFoot)]),ylabel('PAT_{Foot}')
subplot(5,3,9), plot(BP_PP, S_r_Pilt, '.'),xlim([10 80]),ylim([mean(S_r_Pilt)-
3*std(S_r_Pilt) mean(S_r_Pilt)+3*std(S_r_Pilt)]),ylabel('S_{Pilt}')
subplot(5,3,12), plot(BP_PP, a, '.'),xlim([10 80]),ylim([mean(a)-3*std(a)
mean(a)+3*std(a)]),ylabel('a')
subplot(5,3,15), plot(BP_PP, S_r_Sigma, '.'),xlim([10
80]),ylim([mean(S_r_Sigma)-3*std(S_r_Sigma)
mean(S_r_Sigma)+3*std(S_r_Sigma)]),ylabel('S_{Sigma}') ,xlabel('BP PP (mmHg)')

%% Spectral analysis: Coherence estimate
% Resampling of time parameters
R_time_q=1:1:R_time(end); % resampling signal to 1s
SBP_q   = interp1(R_time,SBP,R_time_q,'spline');
```

```
DBP_q   = interp1(R_time,DBP,R_time_q,'spline');
BP_PP_q = interp1(R_time,DBP,R_time_q,'spline');

PATDerMax_q = interp1(R_time,PATDerMax,R_time_q,'spline');
PATFoot_q = interp1(R_time,PATFoot,R_time_q,'spline');
S_r_Pilt_q = interp1(R_time,S_r_Pilt,R_time_q,'spline');
a_q = interp1(R_time,a,R_time_q,'spline');
S_r_Sigma_q = interp1(R_time,S_r_Sigma,R_time_q,'spline');
[C_SBP_PATDerMax,F] = mscohere(SBP_q,PATDerMax_q,hanning(256),128,256,1);
[C_SBP_PATFoot_q,F] = mscohere(SBP_q,PATFoot_q,hanning(256),128,256,1);
[C_SBP_S_r_Pilt_q,F] = mscohere(SBP_q,S_r_Pilt_q,hanning(256),128,256,1);
[C_SBP_S_r_a_q,F] = mscohere(SBP_q,a_q,hanning(256),128,256,1);
[C_SBP_S_S_r_Sigma_q,F] = mscohere(SBP_q,S_r_Sigma_q,hanning(256),128,256,1);

[C_DBP_PATDerMax,F] = mscohere(DBP_q,PATDerMax_q,hanning(256),128,256,1);
[C_DBP_PATFoot_q,F] = mscohere(DBP_q,PATFoot_q,hanning(256),128,256,1);
[C_DBP_S_r_Pilt_q,F] = mscohere(DBP_q,S_r_Pilt_q,hanning(256),128,256,1);
[C_DBP_S_r_a_q,F] = mscohere(DBP_q,a_q,hanning(256),128,256,1);
[C_DBP_S_S_r_Sigma_q,F] = mscohere(DBP_q,S_r_Sigma_q,hanning(256),128,256,1);

[C_BP_PP_q_PATDerMax,F] = mscohere(BP_PP_q,PATDerMax_q,hanning(256),128,256,1);
[C_BP_PP_q_PATFoot_q,F] = mscohere(BP_PP_q,PATFoot_q,hanning(256),128,256,1);
[C_BP_PP_q_S_r_Pilt_q,F] = mscohere(BP_PP_q,S_r_Pilt_q,hanning(256),128,256,1);
[C_BP_PP_q_S_r_a_q,F] = mscohere(BP_PP_q,a_q,hanning(256),128,256,1);
[C_BP_PP_q_S_S_r_Sigma_q,F] =
mscohere(BP_PP_q,S_r_Sigma_q,hanning(256),128,256,1);

figure
plot(F,C_SBP_S_S_r_Sigma_q),xlabel('f (Hz)'),ylabel('Coherence magn.')

figure
subplot(5,3,1), plot(F,C_SBP_PATDerMax),ylabel('C_{SBP PATDerMax}')
subplot(5,3,4), plot(F,C_SBP_PATFoot_q),ylabel('C_{SBP PATFoot}')
subplot(5,3,7), plot(F,C_SBP_S_r_Pilt_q),ylabel('C_{SBP SrPilt}')
subplot(5,3,10), plot(F,C_SBP_S_r_a_q),ylabel('C_{SBP Sra}')
subplot(5,3,13), plot(F,C_SBP_S_S_r_Sigma_q),ylabel('C_{SBP SrSigma}'),xlabel('f
(Hz)')

subplot(5,3,2), plot(F,C_DBP_PATDerMax),ylabel('C_{DBP PATDerMax}')
subplot(5,3,5), plot(F,C_DBP_PATFoot_q),ylabel('C_{DBP PATFoot}')
subplot(5,3,8), plot(F,C_DBP_S_r_a_q),ylabel('C_{DBP SrPilt}')
subplot(5,3,11), plot(F,C_DBP_S_r_a_q),ylabel('C_{DBP Sra}')
subplot(5,3,14), plot(F,C_DBP_S_S_r_Sigma_q),ylabel('C_{SBP SrSigma}'),xlabel('f
(Hz)'),

subplot(5,3,3), plot(F,C_BP_PP_q_PATDerMax),ylabel('C_{DBP PATDerMax}')
subplot(5,3,6), plot(F,C_BP_PP_q_PATFoot_q),ylabel('C_{DBP PATFoot}')
subplot(5,3,9), plot(F,C_BP_PP_q_S_r_Pilt_q),ylabel('C_{DBP SrPilt}')
subplot(5,3,12), plot(F,C_BP_PP_q_S_r_a_q),ylabel('C_{DBP Sra}')
subplot(5,3,15), plot(F,C_BP_PP_q_S_S_r_Sigma_q),ylabel('C_{SBP
SrSigma}'),xlabel('f (Hz)'),
```

```
break
%% Original PPG and fitted model
figure
set(gcf,'Position',[360 -80 560 698])
n=1:length(ppg);
ax1=subplot(5,1,1);
hold on
plot(ppg),grid;
%keyboard

for i=1:length(feet)
    plot(n(feet(i):peak(i)),
ppg_model_Line{i}(1,:),'linewidth',1.5,'color','red');
end
hold off
ylabel('A, mV')
legend('PPG signal','Line model')
box on
ax2=subplot(5,1,2);
plot(Pulse_slope),grid, ylabel('Slope (V/s)'),title('Pulse slope');
ax3=subplot(5,1,3);
plot(Rise_time),grid, ylabel('t_{rise} (s)'),title('Pulse rise time');
ax4=subplot(5,1,4);
plot(Pulse_ampl),grid, ylabel('A (mV)'),title('Pulse amplitude');
ax5=subplot(5,1,5);
plot(SBP),grid,title('Systolic blood pressure');
xlabel('n'), ylabel('SBP, mmHg')
linkaxes([ax2,ax3,ax4,ax5],'x')
%%
figure
hold on
plot(time_ecg,ecg_PAT),title('ECG')
plot(R_time, ecg_PAT(round(R_time*Fs)),'ro')
hold off
```